



Enhanced glass-forming ability of a Sm-based alloy with the addition of La

Yunfei Ji, Shujie Pang, Tao Zhang*

Key Laboratory of Aerospace Materials and Performance (Ministry of Education), School of Materials Science and Engineering, Beijing University of Aeronautics and Astronautics, Beijing 100191, China

ARTICLE INFO

Article history:

Received 3 February 2010

Received in revised form 14 June 2010

Accepted 15 June 2010

Available online 30 June 2010

Keywords:

Metallic glasses

Rapid solidification

Thermal analysis

X-ray diffraction

ABSTRACT

The effects of La on the glass-forming ability (GFA) of a Sm-based alloy were investigated. By partial substitution of Sm with La in $(\text{Sm}_{0.62}\text{Al}_{0.14}\text{Ni}_{0.12}\text{Cu}_{0.12})_{97}\text{Fe}_3$ (at.%) alloy, of which the critical diameter for glass formation is 3 mm, $(\text{Sm}_{0.32}\text{La}_{0.3}\text{Al}_{0.14}\text{Ni}_{0.12}\text{Cu}_{0.12})_{97}\text{Fe}_3$ glassy rods with a diameter up to 10 mm can be fabricated by copper mold casting. The configuration entropy and critical cooling rate of the Sm–La–Al–Ni–Cu–Fe alloy were calculated. It is indicated that the configuration entropy is increased and the critical cooling rate is decreased with the addition of La, implying that the La-containing alloys exhibit higher GFA than that of the La-free Sm–Al–Ni–Cu–Fe alloy. Moreover, with the addition of La, the Sm-based alloys exhibit reduced Gibbs free energy between the liquid phase and the crystalline phase in the supercooled liquid region and stronger liquid behavior, which are also beneficial to the enhanced GFA of the Sm–La–Al–Ni–Cu–Fe alloys.

© 2010 Elsevier B.V. All rights reserved.

1. Introduction

Rare earth metal-based (RE-based) bulk metallic glasses have attracted extensive attention because of their high glass-forming ability (GFA) and novel physical properties, such as special magnetic properties and superplasticity in supercooled liquid region [1–4]. Previous work has preliminarily demonstrated that in contrast with crystalline counterparts, Sm-based metallic glasses have higher coercivity at low temperature and may be utilized for synthesizing superconductor materials [5]. However, the reported Sm-based alloys show limited GFA, and the maximum diameter was only 3–4 mm for the Sm-based bulk metallic glasses (BMGs) [6,7]. Therefore, developing Sm-based BMGs with better GFA is of great importance in science and application of BMGs.

It is known that there should be large atomic size difference and negative heats of mixing among the main constituent elements, which can be defined as dissimilar elements, in good glass-forming alloys [8,9]. During the last decade, many RE-based BMGs with critical diameter in centimeter scale which satisfy this compositional criterion have been discovered [1–4]. Recently, we found that the GFA of some glassy alloys consisting of dissimilar elements can be improved when the elements with similar atomic sizes and electronic configuration to those of the components are added. Using this new approach of the coexistence of similar and dissimilar elements, we have successfully synthesized many BMGs

with superior GFA, e.g., the critical diameter of La–Ce–Al–Co–Cu BMGs reaches up to 32 mm [3,10,11]. Our previous work on the glass formation of $(\text{Sm}_{0.62}\text{Al}_{0.14}\text{Ni}_{0.12}\text{Cu}_{0.12})_{100-x}\text{Fe}_x$ (at.%) alloys revealed that the critical diameters of $\text{Sm}_{62}\text{Al}_{14}\text{Ni}_{12}\text{Cu}_{12}$, $(\text{Sm}_{62}\text{Al}_{14}\text{Ni}_{12}\text{Cu}_{12})_{0.97}\text{Fe}_3$ and $(\text{Sm}_{62}\text{Al}_{14}\text{Ni}_{12}\text{Cu}_{12})_{0.95}\text{Fe}_5$ BMGs are 1, 3 and 2 mm, respectively, indicating that the GFA of $\text{Sm}_{62}\text{Al}_{14}\text{Ni}_{12}\text{Cu}_{12}$ alloy could be enhanced by suitable addition of Fe. To develop Sm-based BMGs with superior GFA, in this paper, we chose $(\text{Sm}_{62}\text{Al}_{14}\text{Ni}_{12}\text{Cu}_{12})_{0.97}\text{Fe}_3$ as base alloy, and add La as a similar element to partially substitute Sm in $(\text{Sm}_{62}\text{Al}_{14}\text{Ni}_{12}\text{Cu}_{12})_{0.97}\text{Fe}_3$ alloy. The effects of La on the GFA of $(\text{Sm}_{62}\text{Al}_{14}\text{Ni}_{12}\text{Cu}_{12})_{0.97}\text{Fe}_3$ alloy are investigated. The origins of the excellent GFA enhanced by La substitution are also systematically investigated from thermodynamic and kinetic aspects.

2. Experimental

$(\text{Sm}_{0.62-x}\text{La}_x\text{Al}_{0.14}\text{Ni}_{0.12}\text{Cu}_{0.12})_{97}\text{Fe}_3$ ($x=0, 0.15$ and 0.3 at.%) alloy ingots were prepared by arc-melting the mixtures of pure Sm (99.9 mass%), La (99.9 mass%), Al (99.99 mass%), Ni (99.99 mass%), Cu (99.99 mass%) and Fe (99.99 mass%) metals in a high-purity argon atmosphere. The ingots were remelted at least three times to insure their chemical homogeneity. From the master alloys, cylindrical rods were fabricated by copper mold casting under a high-purity argon atmosphere. Cross sections of the as-cast rods were examined by X-ray diffraction (XRD) using a Rigaku D/max 2200 pc automatic X-ray diffractometer with $\text{Cu K}\alpha$ radiation to study the structure. The $(\text{Sm}_{0.32}\text{La}_{0.3}\text{Al}_{0.14}\text{Ni}_{0.12}\text{Cu}_{0.12})_{97}\text{Fe}_3$ glassy alloy with a diameter of 10 mm was observed with JEM-2100F transmission electron microscope (TEM) at an operating voltage of 200 kV. The thermal stability associated with glass transition, supercooled liquid region, crystallization and melting behavior was examined by NETZSCH DSC 404C differential scanning calorimetry (DSC) at a heating rate of 0.33 K/s. The apparent activation energies of the first-stage crystallization and the fragility indexes of these glassy alloys were also studied by the DSC at the heating rates ranging from 0.083 to 0.83 K/s.

* Corresponding author. Tel.: +86 10 8231 6192; fax: +86 10 8231 4869.
E-mail address: zhangtao@buaa.edu.cn (T. Zhang).

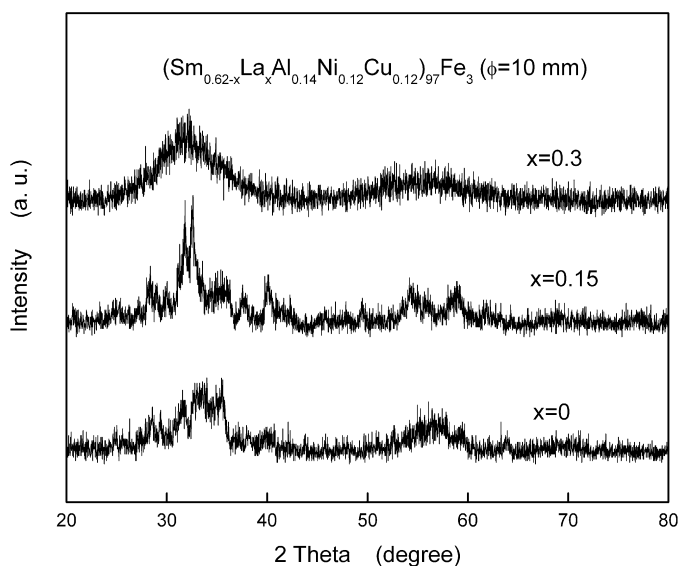


Fig. 1. XRD patterns of $(\text{Sm}_{0.62-x}\text{La}_x\text{Al}_{0.14}\text{Ni}_{0.12}\text{Cu}_{0.12})_{97}\text{Fe}_3$ ($x=0, 0.15$ and 0.3) cast rods of 10 mm in diameter.

3. Results and discussion

XRD patterns of the as-cast $(\text{Sm}_{0.62-x}\text{La}_x\text{Al}_{0.14}\text{Ni}_{0.12}\text{Cu}_{0.12})_{97}\text{Fe}_3$ ($x=0, 0.15$ and 0.3) alloys (denoted as SL0, SL15 and SL30, respectively, for convenience in the following text) with a diameter of 10 mm are shown in Fig. 1. The diffraction peaks corresponding to crystalline phases can be observed for the SL0 and SL15 alloys. However, SL30 alloy with a diameter of 10 mm exhibits broad diffraction maxima without crystalline Bragg peaks, which is characteristic for glassy alloys. In addition, the high-resolution transmission electron microscope image (HRTEM) (Fig. 2) of the SL30 sample with a diameter of 10 mm shows no distinguishable crystallites. The corresponding selected area electron diffraction (SAED) pattern (as shown in the inset of Fig. 2) exhibits only a halo ring, which is inherent to a glassy phase, confirming that the SL30 sample of 10 mm

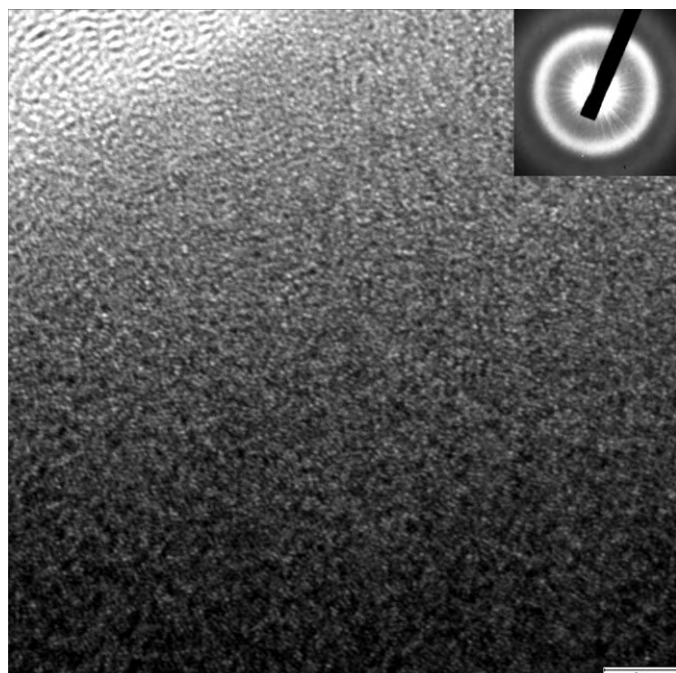


Fig. 2. HRTEM image and SAED pattern (inset) of SL30 cast rod of 10 mm in diameter.

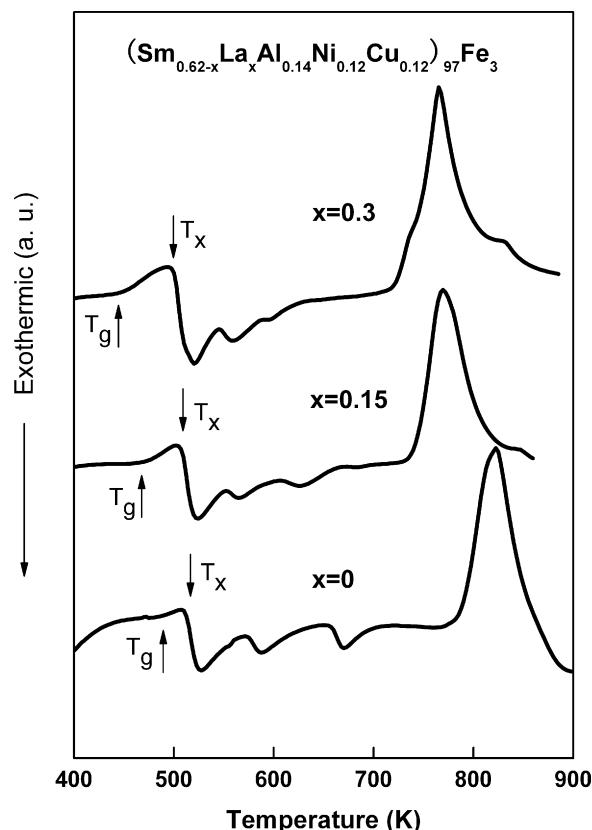


Fig. 3. DSC traces of $(\text{Sm}_{0.62-x}\text{La}_x\text{Al}_{0.14}\text{Ni}_{0.12}\text{Cu}_{0.12})_{97}\text{Fe}_3$ ($x=0, 0.15$ and 0.3) BMG with the critical diameters.

in diameter consists of glassy structure. Moreover, we have confirmed that the critical diameters of SL0 and SL15 BMGs are 3 and 5 mm, respectively. These results indicate that the addition of La considerably enhances the GFA of the Sm-based alloy.

The DSC traces of SL0 to SL30 BMGs with the critical diameters are shown in Fig. 3. Glass transition followed by supercooled liquid region and several crystallization peaks can be observed on the curves. The glass transition temperature (T_g), onset temperature of crystallization (T_x) and melting temperature (T_m) determined from the DSC traces as well as the supercooled liquid region ($\Delta T_x = T_x - T_g$) and reduced glass transition temperature ($T_{rg} = T_g/T_m$) are listed in Table 1. It has been proposed that for a given alloy system, the increase in ΔT_x and T_{rg} may reflect the enhancement in GFA [12–14]. In the present study, the highest ΔT_x value of SL30 metallic glass can give a good explanation for the difference in GFA between SL0 and SL30 alloys. It is noted that the criterion T_{rg} is not effective for evaluating the GFA of the Sm–La–Al–Ni–Cu–Fe BMG alloys.

The critical cooling rate (R_c) estimated by theoretical calculation is an ideal parameter employed for the explanation of GFA [15,16]. That is, alloys with higher GFA always have lower critical cooling rate. In accordance with the classical crystallization theory, the R_c of metallic glasses can be represented as [15]:

$$R_c = Z \frac{k_B T_m^2}{a^3 \eta_{T=T_m}} \exp \left[f_1 \left(\frac{\Delta H - T_m \Delta S_{\text{ideal}}}{300R} \right) - f_2 \left(\frac{T_m S_\sigma}{300R} \right) \right] \quad (1)$$

where Z is a constant, taken as 2×10^{-6} , k_B the Boltzmann constant, a the average interatomic distance, η the viscosity, ΔH the mixing enthalpy of the system, ΔS_{ideal} the ideal configurational entropy, S_σ the mismatch term of entropy and R the gas constant. By the method of least-squares, f_1 and f_2 were calculated to be 0.75 and 1.2, respectively [15].

Table 1

Glass transition temperature (T_g), crystallization temperature (T_x), supercooled liquid region ($\Delta T_x = T_x - T_g$), melting temperature (T_m) and reduced glass transition temperature ($T_{rg} = T_g/T_m$) for ($\text{Sm}_{0.62-x}\text{La}_x\text{Al}_{0.14}\text{Ni}_{0.12}\text{Cu}_{0.12}$) $_{97}\text{Fe}_3$ ($x = 0, 0.15$ and 0.3) metallic glasses with their critical diameters taken from the DSC traces measured at a heating rate of 0.33 K/s .

| Alloy | T_g (K) | T_x (K) | ΔT_x (K) | T_m (K) | $T_{rg} = T_g/T_m$ |
|---|-----------|-----------|------------------|-----------|--------------------|
| ($\text{Sm}_{0.62}\text{Al}_{0.14}\text{Ni}_{0.12}\text{Cu}_{0.12}$) $_{97}\text{Fe}_3$ | 482 | 513 | 31 | 787 | 0.61 |
| ($\text{Sm}_{0.47}\text{La}_{0.15}\text{Al}_{0.14}\text{Ni}_{0.12}\text{Cu}_{0.12}$) $_{97}\text{Fe}_3$ | 474 | 509 | 35 | 743 | 0.64 |
| ($\text{Sm}_{0.32}\text{La}_{0.3}\text{Al}_{0.14}\text{Ni}_{0.12}\text{Cu}_{0.12}$) $_{97}\text{Fe}_3$ | 450 | 501 | 51 | 720 | 0.62 |

According to the regular solution model, ΔH and ΔS^{ideal} are defined as Eqs. (2) and (3) for the multi-component systems with N elements [15]:

$$\Delta H = \sum_{i=1, i \neq j}^N \Omega_{ij} c_i c_j \quad (2)$$

$$\Delta S^{\text{ideal}} = -R \sum_{i=1}^N (c_i \ln c_i) \quad (3)$$

where R is the gas constant, c_i the mole fraction of i , Ω_{ij} the regular solution interaction parameter between i and j elements, and can be calculated as:

$$\Omega_{ij} = 4\Delta H_{AB}^{\text{mix}} \quad (4)$$

The relation is due to definition in Eq. (2) at the equal-atomic composition in a binary A–B system and $\Delta H_{AB}^{\text{mix}}$ is the mixing enthalpy of the binary A–B system. In the present study, as La and Sm are similar elements with similar atomic size and chemical properties, Ω_{ij} and ΔH are nearly the same for SL0, SL15 and SL30 alloys according to Eqs. (4) and (2). Comparing with SL0 alloy, it is reasonable to assume that SL15 and SL30 alloys possess similar values of a , $\eta_{T=T_m}$ and S_σ . Therefore, T_m and ΔS^{ideal} could be treated to be the primary factors resulted in the difference in R_c among SL0, SL15 and SL30 alloys. From Table 1, it is seen that the T_m decreases with the increase in La content in ($\text{Sm}_{0.62-x}\text{La}_x\text{Al}_{0.14}\text{Ni}_{0.12}\text{Cu}_{0.12}$) $_{97}\text{Fe}_3$ alloys. The ideal configuration entropy calculated from Eq. (3) increases with La content increasing from 0 to 0.3. Consequently, the R_c decreases with the addition of La, indicating that the La-containing alloys have higher GFA than the La-free Sm-based alloy, which is in agreement with the experimental results in the present work.

It is known that in a specified alloy system, a smaller Gibbs free energy difference (ΔG) between liquid and crystal phases in the supercooled liquid region appears to be a contributing factor to the higher GFA [17,18]. It has been reported that the ΔG can be calculated using the following formula according to ref. [17]:

$$\Delta G = \frac{\Delta H_f \Delta T}{T_m} - \tau \Delta S_f \left[\Delta T - T \ln \left(\frac{T_m}{T} \right) \right] \quad (5)$$

where ΔH_f is the fusion enthalpy, ΔT equals to $T_m - T$, ΔC_p the difference in the specific heat capacities between liquid and crystal phases, ΔS_f equals to $\Delta H_f/T_m$, and τ the proportionality coefficient, usually taken as 0.8 for metallic glass-forming liquids [17,18].

At $0.8T_m$, which is a temperature for T used in the previous research [18], ΔG can be represented as:

$$\Delta G = 0.1828\Delta H_f \quad (6)$$

ΔG is calculated to be 1.58 and 1.39 kJ/mol for SL0 and SL30 alloys, respectively. Thus the lower Gibbs free energy difference between the liquid and crystalline phases in the supercooled liquid region induced by La addition may reflect the enhanced GFA.

In order to examine the thermal stability associated with crystallization kinetics for the Sm–La–Al–Ni–Cu–Fe glassy alloys, the apparent activation energies of the first-stage crystallization under

continuous heating conditions are estimated by the Kissinger equation [19–22]:

$$\ln \frac{T^2}{Q} = \frac{\Delta E}{RT} + A \quad (7)$$

where Q is the heating rate, ΔE the apparent activation energy for the first-stage crystallization, T the peak temperature of the first-stage crystallization and A constant. By plotting $\ln(T^2/Q)$ versus $1/T$, an approximately straight line with a slope of $\Delta E/R$ can be obtained and so that ΔE can be calculated. Fig. 4 shows the Kissinger plots for SL0, SL15 and SL30 metallic glasses, from which the crystallization activation energies of these three metallic glasses are determined to be 217.4, 163.2 and 151.9 kJ/mol, respectively.

According to Angell, glasses can be largely classified into two groups: strong glasses and fragile glasses [23]. In general, the strong glasses exhibit smaller change in viscosity during heating than the fragile glasses, indicating that the stronger glasses have more dense packed structure [23]. The fragility of a glass can be described by a Vogel–Fulcher–Tamman (VFT) relation and can be quantitatively assessed by the fragility index m . Generally, BMGs exhibit analogous m values in the range of 25–60 and smaller m means stronger bonding nature of atoms in the liquid and higher GFA for the systems with nearly the same T_{rg} values [24,25].

In the present study, the dependence of the glass transition temperature on the heating rate Q is evaluated in terms of the VFT equation expressed in the form [26,27]:

$$\ln Q = \ln B - \frac{DT_0}{T_g - T_0} \quad (8)$$

where T_0 is the asymptotic value of T_g , usually being approximated as the onset of glass transition in the limit of infinitely slow cooling/heating rate, D the fragility parameter and B an adjustable parameter. The fitting of the experimental data shown in Fig. 5 is performed based on the Eq. (8) with three adjustable VFT param-

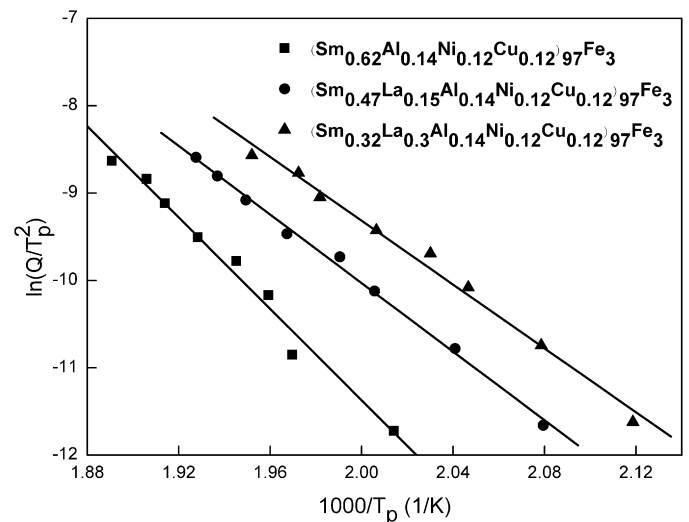


Fig. 4. Kissinger plots of the DSC data for ($\text{Sm}_{0.62-x}\text{La}_x\text{Al}_{0.14}\text{Ni}_{0.12}\text{Cu}_{0.12}$) $_{97}\text{Fe}_3$ ($x = 0, 0.15$ and 0.3) BMG with a diameter of 2 mm.

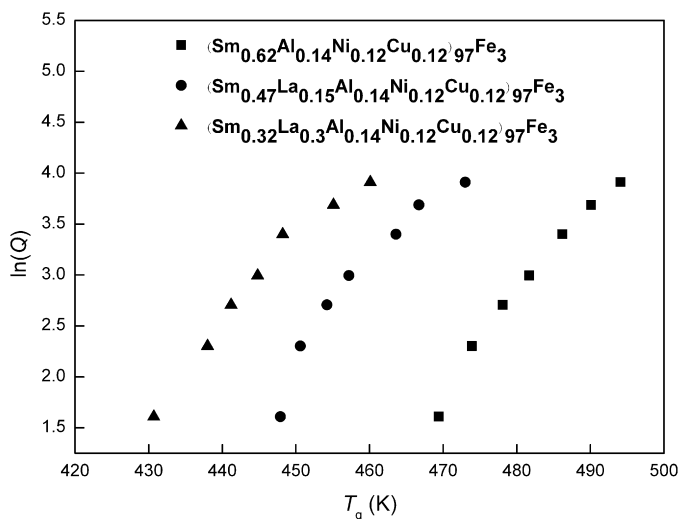


Fig. 5. Glass transition temperature (T_g) vs. $\ln(Q)$ for the $(\text{Sm}_{0.62-x}\text{La}_x\text{Al}_{0.14}\text{Ni}_{0.12}\text{Cu}_{0.12})_{97}\text{Fe}_3$ ($x=0, 0.15$ and 0.3) BMG with a diameter of 2 mm.

eters: B , D and T_0 . Using the VFT fitting parameters, the fragility index m at the given T_g can be calculated by the following relation [26,27]:

$$m = \frac{DT_0T_g}{(T_g - T_0)^2 \ln 10} \quad (9)$$

According to Eq. (9), the fragility index m of SL0 alloy equals to 33.1, higher than 31.6 of SL15 alloy and 30.8 of SL30 alloy, indicating that the fragility index decreases with the addition of La. Therefore, the stronger liquid behaviors and more random packed atomic structures with relatively small amount of free volume and stronger chemical short-range ordering also contribute to the enhanced GFA of the Sm–La–Al–Ni–Cu–Fe alloys by the addition of La.

4. Conclusions

By partial substitution of Sm with La in $(\text{Sm}_{0.62-x}\text{La}_x\text{Al}_{0.14}\text{Ni}_{0.12}\text{Cu}_{0.12})_{97}\text{Fe}_3$ ($x=0, 0.15$ and 0.3) alloys, the GFA is enhanced. Sm-rich $(\text{Sm}_{0.32}\text{La}_{0.3}\text{Al}_{0.14}\text{Ni}_{0.12}\text{Cu}_{0.12})_{97}\text{Fe}_3$ glassy rod with a diameter up to 10 mm can be fabricated by

copper mold casting. With the increase in La content in the range of $0 \leq x \leq 0.3$, the ideal configuration entropy of the alloys is increased and the critical cooling rate is decreased, indicating the enhancement of the GFA. Moreover, with the addition of La, the Sm–La–Al–Ni–Cu–Fe alloys exhibit reduced Gibbs free energy between the liquid phase and the crystalline phase in supercooled liquid region and lower fragility index, which are also beneficial to the glass formation.

Acknowledgements

This work was supported by Natural Science Foundation of China (Nos. 50631010 and 50771006), National Basic Research Program of China (2007CB613900) and Program for NCET (NCET-07-0041).

References

- [1] A. Inoue, T. Zhang, A. Takeuchi, W. Zhang, Mater. Trans. JIM 37 (1996) 636–640.
- [2] Y. Zhang, H. Tan, Y. Li, Mater. Sci. Eng. A 375 (2004) 436–439.
- [3] T. Zhang, R. Li, S.J. Pang, J. Alloys Compd. 483 (2009) 60–63.
- [4] Z.P. Lu, X. Hu, Y. Li, S.C. Ng, Mater. Sci. Eng. A 304–306 (2001) 679–682.
- [5] J. Guo, X.F. Bian, T. Lin, Y. Zhao, T.B. Li, B. Zhang, B.A. Sun, Intermetallics 15 (2007) 929–933.
- [6] J. Wu, Q. Wang, F. Chen, Y.M. Wang, J.B. Qiang, C. Dong, Intermetallics 15 (2007) 652–654.
- [7] G.J. Fan, W. Löser, S. Roth, J. Eckert, Acta Mater. 48 (2000) 3823–3831.
- [8] A. Inoue, Mater. Trans. JIM 36 (1995) 866–875.
- [9] H.S. Chen, Chin. J. Phys. 28 (1990) 407–425.
- [10] R. Li, S.J. Pang, C.L. Ma, T. Zhang, Acta Mater. 55 (2007) 3719–3726.
- [11] R. Li, Q. Yang, S.J. Pang, C.L. Ma, T. Zhang, J. Alloys Compd. 450 (2008) 181–184.
- [12] Z.P. Lu, C.T. Liu, Acta Mater. 50 (2002) 3501–3512.
- [13] Z.P. Lu, C.T. Liu, Phys. Rev. Lett. 91 (2003) 115505.
- [14] I.A. Figueroa, H.A. Davies, I. Todd, J. Alloys Compd. 434–435 (2007) 164–166.
- [15] A. Takeuchi, A. Inoue, Mater. Sci. Eng. A 304–306 (2001) 446–451.
- [16] J. Torrens-Serra, J. Rodriguez-Viejo, M.T. Clavaguera-Mora, Scripta Mater. 61 (2009) 879–882.
- [17] F.Q. Guo, S.J. Poon, G.J. Shiflet, Appl. Phys. Lett. 83 (2003) 2575–2577.
- [18] J. Shen, Q.J. Chen, J.F. Sun, H.B. Fan, G. Wang, Appl. Phys. Lett. 86 (2005) 151907.
- [19] Q.J. Chen, H.B. Fan, J. Shen, J.F. Sun, Z.P. Lu, J. Alloys Compd. 407 (2006) 125–128.
- [20] B. Yao, K. Zhang, H. Tan, Y. Li, J. Non-Cryst. Solids 354 (2008) 970–974.
- [21] Z. Śniadecki, B. Idzikowski, J. Non-Cryst. Solids 354 (2008) 5159–5161.
- [22] I. Kokanovic, A. Tonejc, Mater. Sci. Eng. A 373 (2004) 26–32.
- [23] C.A. Angell, Science 267 (1995) 1924–1935.
- [24] E.S. Park, J.H. Na, D.H. Kim, Appl. Phys. Lett. 91 (2007) 031907.
- [25] O.N. Senkov, Phys. Rev. B 76 (2007) 104202.
- [26] W.M. Wang, A. Gebert, S. Roth, U. Kuehn, L. Schultz, Intermetallics 16 (2008) 267–272.
- [27] Z. Zhang, W.H. Wang, Y. Hirotsu, Mater. Sci. Eng. A 385 (2004) 38–43.